

**OAK RIDGE NATIONAL LABORATORY**  
 operated by  
**UNION CARBIDE CORPORATION**  
 NUCLEAR DIVISION  
 for the  
**U.S. ATOMIC ENERGY COMMISSION**



ORNL-TM-2125

CENTRAL RESEARCH LIBRARY  
 DOCUMENT COLLECTION

LOCKHEED MARTIN ENERGY RESEARCH LIBRARIES



3 4456 0513020 2

**EFFECTS OF STAGE TEMPERATURE DROP ON THERMAL STRESSES  
 IN REPRESENTATIVE CESIUM AND POTASSIUM TURBINES**

OAK RIDGE NATIONAL LABORATORY  
 CENTRAL RESEARCH LIBRARY  
 DOCUMENT COLLECTION  
**LIBRARY LOAN COPY**

DO NOT TRANSFER TO ANOTHER PERSON

If you wish someone else to see this  
 document, send in name with document  
 and the library will arrange a loan.

UCN-7969  
 (3 3+67)

**NOTICE** This document contains information of a preliminary nature and was prepared primarily for internal use at the Oak Ridge National Laboratory. It is subject to revision or correction and therefore does not represent a final report.

LEGAL NOTICE

This report was prepared as an account of Government sponsored work. Neither the United States, nor the Commission, nor any person acting on behalf of the Commission:

- A. Makes any warranty or representation, expressed or implied, with respect to the accuracy, completeness, or usefulness of the information contained in this report, or that the use of any information, apparatus, method, or process disclosed in this report may not infringe privately owned rights; or
- B. Assumes any liabilities with respect to the use of, or for damages resulting from the use of any information, apparatus, method, or process disclosed in this report.

As used in the above, "person acting on behalf of the Commission" includes any employee or contractor of the Commission, or employee of such contractor, to the extent that such employee or contractor of the Commission, or employee of such contractor prepares, disseminates, or provides access to, any information pursuant to his employment or contract with the Commission, or his employment with such contractor.

Contract No. W-7405-eng-26

REACTOR DIVISION

EFFECTS OF STAGE TEMPERATURE DROP ON THERMAL STRESSES  
IN REPRESENTATIVE CESIUM AND POTASSIUM TURBINES

M. E. LaVerne      T. T. Robin

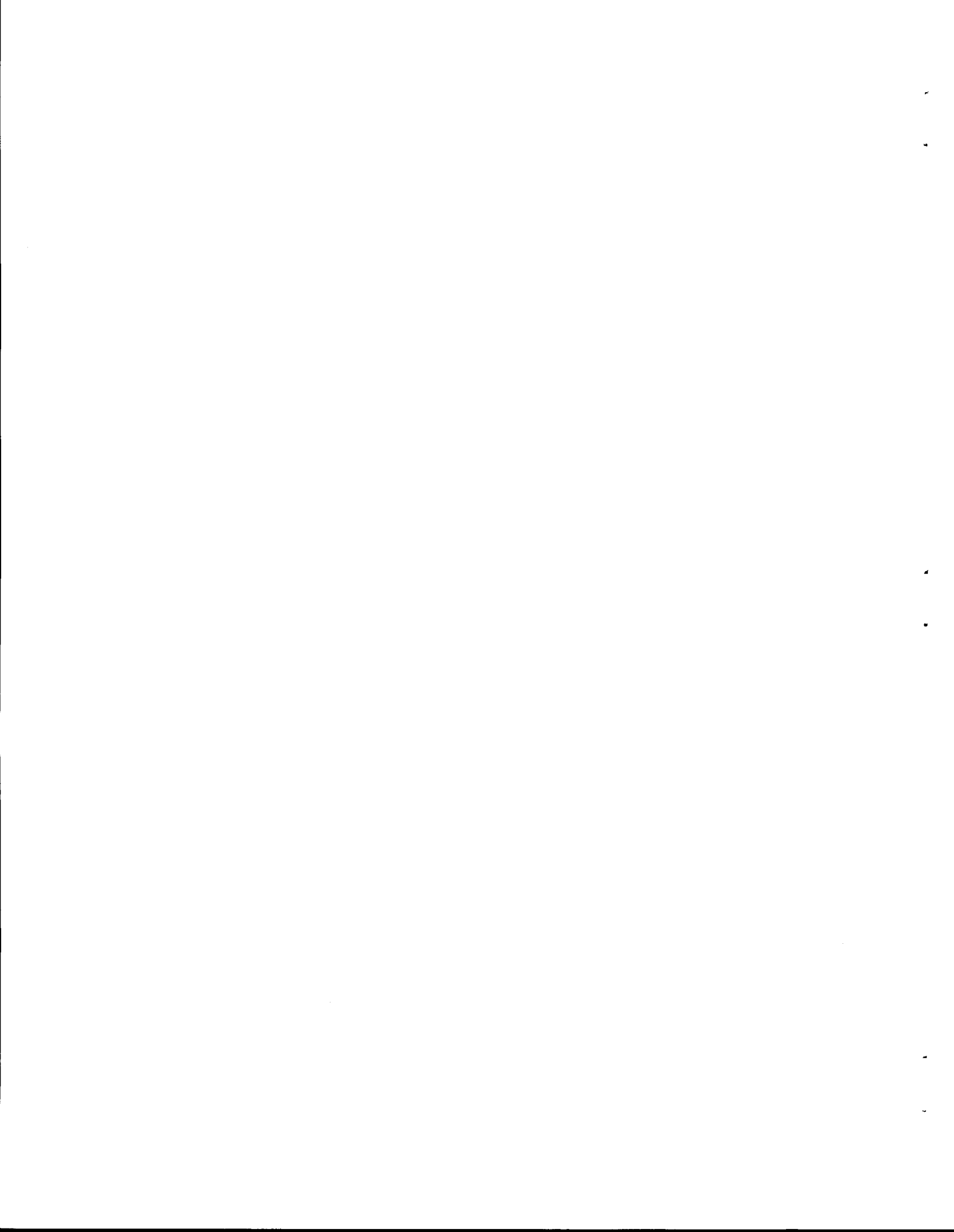
NOVEMBER 1968

OAK RIDGE NATIONAL LABORATORY  
Oak Ridge, Tennessee  
operated by  
UNION CARBIDE CORPORATION  
for the  
U.S. ATOMIC ENERGY COMMISSION

LOCKHEED MARTIN ENERGY RESEARCH LIBRARIES

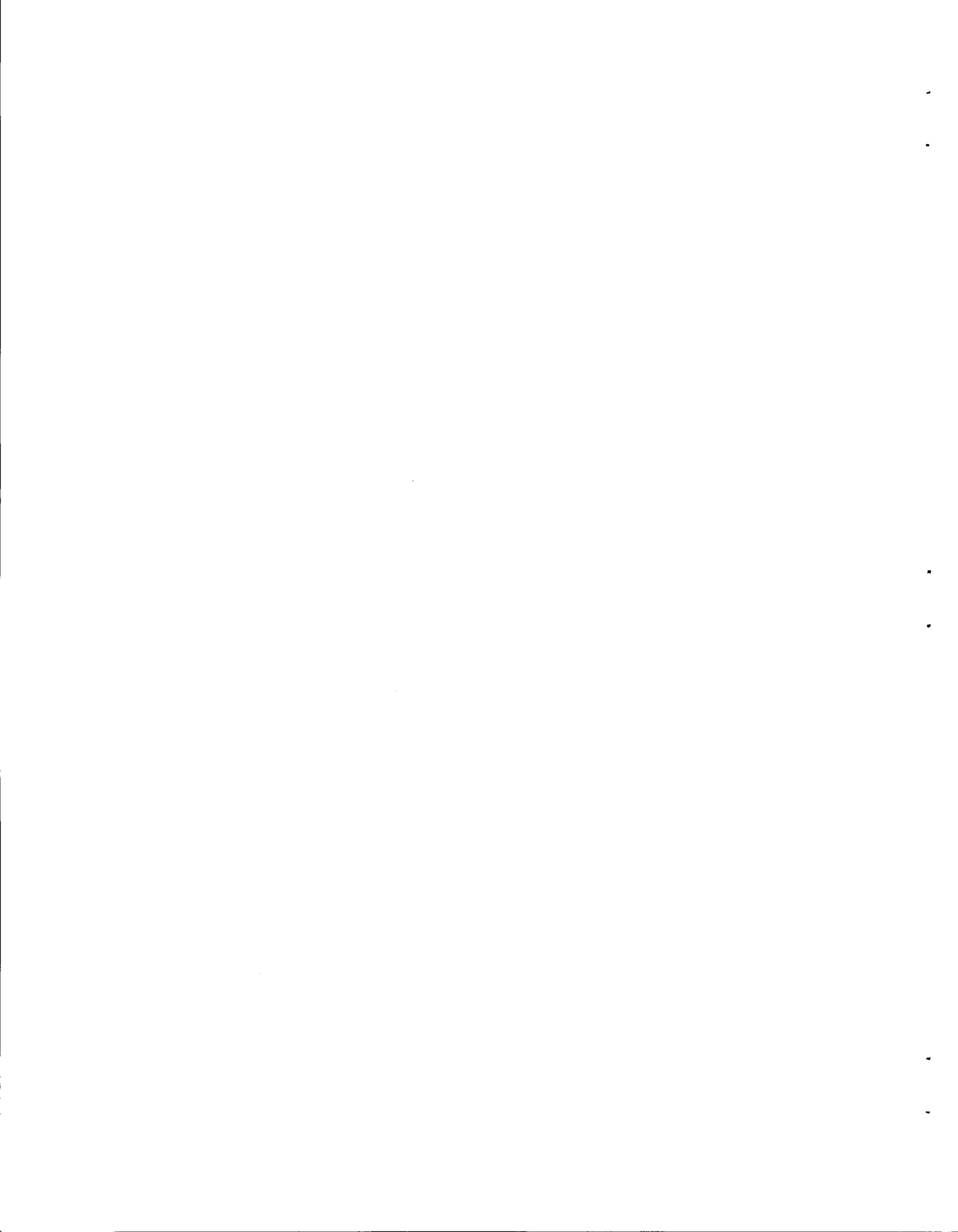


3 4456 0513020 2



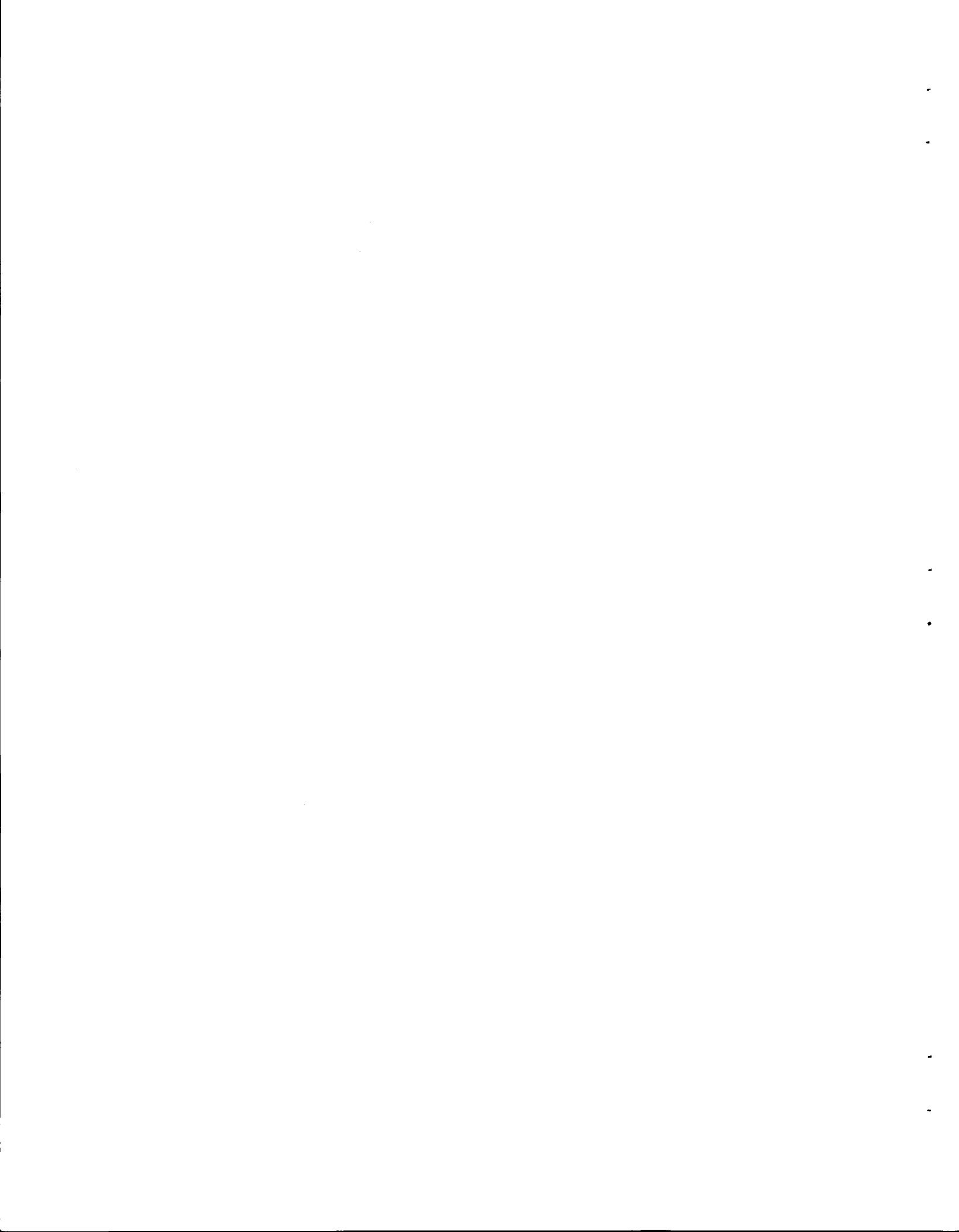
## FOREWORD

This report summarizes analyses of the temperature distributions and thermal stresses in an analytical comparison of cesium and potassium as working fluids for Rankine cycle space power plants. The work was conducted by the Oak Ridge National Laboratory for NASA under AEC Interagency Agreement 40-98-66, NASA Order W-12,353 under the technical management of A. P. Fraas of the Oak Ridge National Laboratory. Project management for NASA was performed by S. V. Manson of NASA Headquarters.



## CONTENTS

	<u>Page</u>
ABSTRACT .....	1
INTRODUCTION .....	1
ANALYSIS .....	3
Temperature Distribution .....	3
Calculational Procedure .....	3
Stress Analysis .....	6
Order of Magnitude Estimates .....	6
Hubs and Seals .....	6
Wheels .....	6
Bolt .....	6
Stress Calculation by the Finite-Element Method .....	7
RESULTS .....	7
Temperature Distributions .....	7
Stresses .....	13
Hubs and Seals .....	13
Wheels .....	13
Bolt .....	15
REFERENCES .....	17



EFFECTS OF STAGE TEMPERATURE DROP ON THERMAL STRESSES  
IN REPRESENTATIVE CESIUM AND POTASSIUM TURBINES

M. E. LaVerne    T. T. Robin

Abstract

Turbine reference designs for both potassium and cesium systems were analyzed for thermal stresses. Detailed temperature distributions for the rotors were calculated with a finite-difference computer code. Order of magnitude thermal stress estimates indicated that the most severe stresses would occur in the hub region between the first stage rotor and its adjacent bearing in the four-bearing machines, and that these stresses would be well below the 20,000 psi maximum allowable for TZM at 2100°F. Detailed analyses of these components using a code based on the finite element method showed actual thermal stresses in this region of the order of 2000 psi. Order of magnitude estimates for the stators and other components also indicated thermal stresses below the maximum allowable.

---

INTRODUCTION

A number of authorities have pointed out that the thermodynamic properties of cesium afford the turbine designer some degrees of freedom that are not available with potassium, and that these may make possible lighter, simpler, more reliable turbines. The problems involved have been examined by a number of organizations.<sup>1-3</sup> Some have concluded that there is little difference between the systems, whereas others have concluded that there would be a major advantage to the use of cesium. The Oak Ridge National Laboratory was asked by NASA to undertake a comparative study of the two systems with the objective of highlighting the principal differences that result from the use of one fluid or the other, and the principal advantages and disadvantages of each from the standpoint of the design and development of the individual components and the complete integrated systems (AEC Interagency Agreement 40-98-66, NASA Order W-12,353).

Six reference design 300 Kw turbines, three cesium and three potassium, were developed from a common set of design precepts and a series of parametric studies.<sup>1</sup> A major consideration in the development of the

layouts for these turbines was to keep thermal stresses as low as possible. However, it was evident that substantial thermal stresses would tend to occur. Of the six reference designs two turbines were chosen for detailed thermal stress analysis because they inherently had the highest thermal gradients and thermal stresses. These were the two-bearing, two-stage cesium machine and the four-bearing, five-stage potassium machine. The thermal stresses in the other four reference designs should be less severe.

At full power, each of the two turbines analyzed has an inlet temperature of 2150°F and an exhaust temperature of 1330°F. The interstage temperature difference thus is about 165°F for the potassium turbine and 410°F for the cesium turbine. Because of this larger temperature difference, the cesium turbine would appear to present a more severe thermal stress problem than the potassium turbine.

To balance the axial pressure forces acting on the rotor, the designs call for the inlet end of the rotor shaft to be exposed to vapor at exhaust pressure. This subjects the first shaft seal to the difference between the exhaust temperature and the first-stage nozzle outlet temperature. For the four-bearing potassium turbine, this difference amounts to 660°F, whereas for the two-bearing cesium turbine it is 410°F, thus indicating that the former is the more severely stressed.

In order to assess the relative importance of the above conflicting factors, a finite-difference computer code was written for determining detailed temperature distributions in the turbine rotors. Order of magnitude stress estimates based on the resulting temperature distributions then indicated that the most severely stressed components would be in the potassium turbine and have an upper limit stress below the 20,000 psi maximum allowable for TZM at 2100°F. Detailed analysis of the same components, using the SAFE-PCRS code,<sup>4</sup> showed that the actual stresses were of the order of 2000 psi.

The quite complex geometry of the turbine casing precluded (at least, within the allotted time) determining casing temperature distributions in the detail necessary for the proper application of the SAFE-PCRS code. Consequently, the efforts here were confined to obtaining order of magnitude

stress estimates for casing elements such as the seals. These estimates indicated stresses below the allowable maximum.

The stagnation temperature rise in the vapor at the turbine rotor blade leading edge produces a highly localized heating effect. For example, if the blade leading edge were approximated as cylindrical with a radius of 0.010 in., the temperature spike would occur over a distance of about 0.005 in. The effect of this impact temperature rise in the vapor on the temperature distribution and, hence, the thermal stress in the rotor blades is unresolved at this time. However, there is reason to believe that the liquid film on the blades, important in minimizing the erosion induced by droplet impact,<sup>5</sup> would also serve to diminish the effect of the impact temperature spike. Firstly, the presence of this highly conductive film would tend to smear out the temperature spike. Secondly, re-evaporation from the film would help to reduce heat penetration to the blade surface.

## ANALYSIS

### Temperature Distribution

#### Calculational Procedure

The actual geometry of the turbine rotors was approximated as indicated in Fig. 1 for the two-stage Cs turbine. Each component of the rotor (bolt, hubs, wheels) was considered to be built up from a number of circular rings in intimate contact, each ring having the same rectangular cross section in the r-z plane. A characteristic temperature at a central nodal point was associated with each ring element.

For each nodal point, one or more of the following steady-state heat flow equations was written. The radial direction is indicated here; a similar set was, of course, written for the axial direction. For conduction within a component,

$$q_k = kA_r \Delta t / \Delta r ; \quad (1)$$

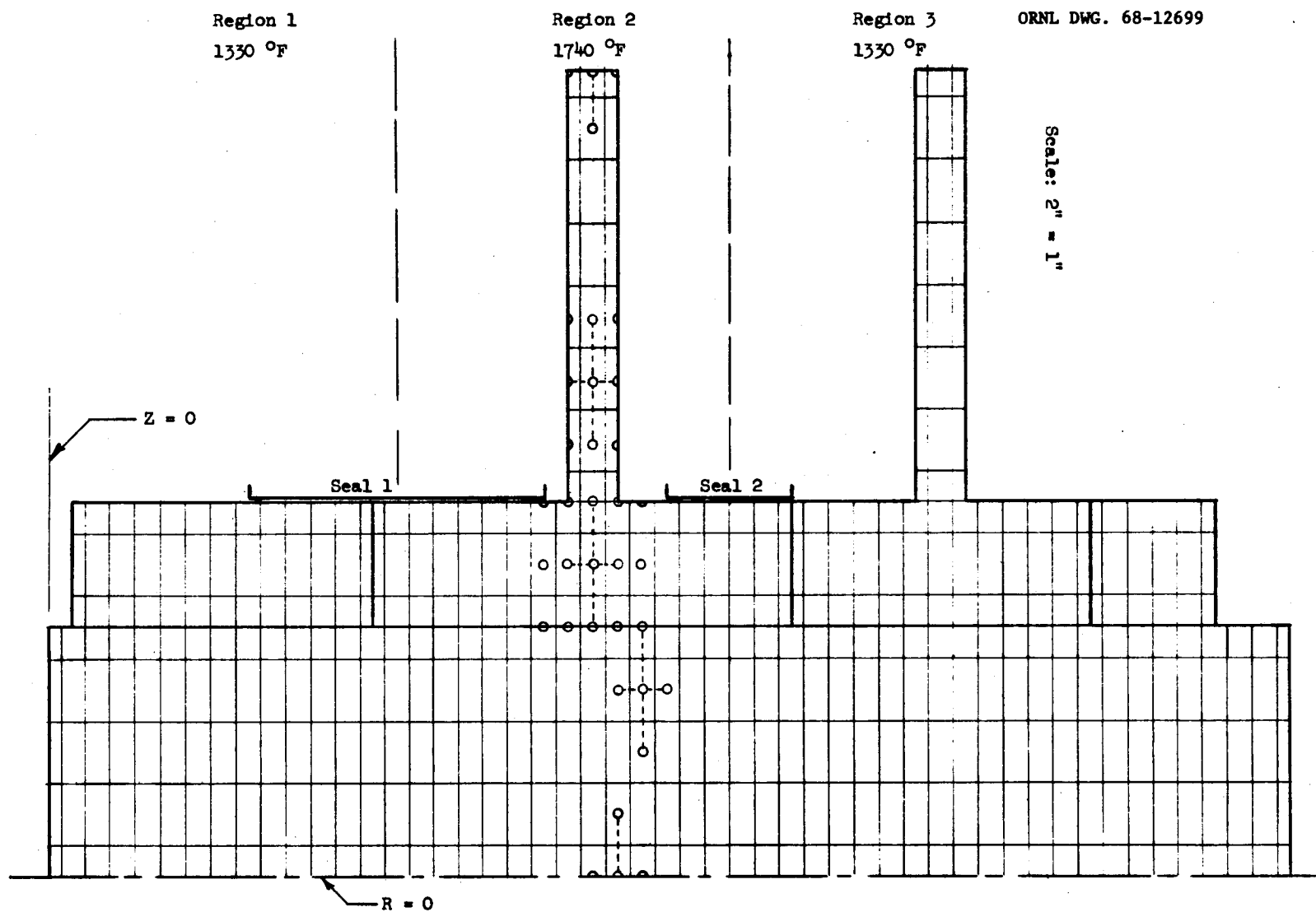


Fig. 1. Finite-Difference Grid for Calculation of Temperature Distribution in 2-Stage Cs Turbine Rotor.

for convection to the vapor,

$$q_h = h A_r \Delta t ; \quad (2)$$

for transfer across a contact resistance, such as between the bolt and a hub,

$$q_c = h_c A_r \Delta t . \quad (3)$$

The radial and axial heat flow areas,  $A_r$  and  $A_z$ , respectively, are equal to the corresponding surface areas of the ring elements. They are, therefore, functions of the radial position of the nodal point.

In each of the regions indicated in Fig. 1, the corresponding rotor components were considered to be exposed to a constant vapor temperature, except under the seals. The vapor temperature in the annular space between hubs and seals was taken as varying linearly in the axial direction. The temperatures at the seal ends were, of course, those in the regions separated by the seal.

By summing the heat flow contributions to each nodal point from its neighboring points and equating this sum to zero, relations were obtained for the steady-state nodal point temperatures in terms of adjacent temperatures, heat flow areas, and coefficients. Several typical point patterns for nodes and their (generally) four neighbors are shown in Fig. 1.

The resulting set of linear equations was then iterated, starting from an initial assumed temperature distribution. Iteration was terminated when the maximum temperature change between iterations fell below a pre-set value for every nodal point.

An estimate of the effect of local heating from the vapor stagnation temperature at the turbine blade leading edge was obtained by a perturbation calculation. The static vapor temperatures adjacent to the upstream corner of a turbine wheel were replaced by the total, or stagnation, temperature resulting from slowing the vapor stream from spouting velocity to wheel tip speed.

## Stress Analysis

### Order of Magnitude Estimates

Hubs and Seals. Both the hubs and seals are in the form of cylindrical shells wherein the principal temperature variation lies in the axial direction. Timoshenko<sup>6</sup> gives, for the thermal stress in cylindrical shells with the temperature varying linearly in the axial direction,

$$\sigma_{\max} = 6M/h^2 \quad (4)$$

where

$$M = -\beta D \alpha a \Delta t / 2b$$

$$\beta^4 = 3(1 - \nu^2) / a^2 h^2$$

and

$$D = Eh^3 / 12(1 - \nu^3).$$

With  $\nu = 0.3$ , we then have for the thermal stress estimator

$$\sigma_{\max} = -0.33 E \alpha \Delta t \sqrt{ah/b} . \quad (5)$$

Wheels. In contrast to the hubs and seals, the temperature variation in the turbine wheels is predominantly in the radial direction, the axial temperature being substantially constant. For a radial temperature variation, we have for the stress estimator<sup>7</sup>

$$\sigma_{\max} = E \alpha \Delta t / 2(1 - \nu). \quad (6)$$

Bolt. In general, axial temperature variations do not induce large thermal stresses in long cylinders except in the neighborhood of sharp changes in the temperature gradient. For such a neighborhood, we have

$$\sigma_{\max} = E \alpha \Delta t / 2 \quad (7)$$

as a conservative estimate of the thermally induced stresses.<sup>7</sup> The temperature difference,  $\Delta t$ , is the maximum value in the neighborhood of a sharp change in the gradient and is measured over a length of about one bolt diameter.

## Stress Calculation by the Finite-Element Method<sup>8</sup>

In the finite element method, the basic concept entails the idealization of the actual structure into a finite number of discrete structural elements, these elements being interconnected at a finite number of nodal points. As used in Refs. 4 and 8, these elements are complete rings of triangular cross section. Figures 2 and 3 illustrate the finite-element subdivision of two of the components of the five-stage potassium turbine. Enough of the nodes and elements have been labeled to show the numbering scheme.

Under the influence of imposed loads and thermal strains, those displacements satisfying the nodal point equilibrium and compatibility conditions are determined. From these displacements, the strains and, thence, the stresses may be determined.

Because of the rather large number of equations to be solved (of the order of 1000), it is necessary to resort to a digital computer solution of the problem. Reference 4 describes a computer program for the axisymmetric stress analysis of composite bodies. This program, SAFE-PCRS, was used for a partial analysis of the 5-stage potassium turbine. Lack of time and funding precluded a complete analysis.

## RESULTS

### Temperature Distributions

Table 1 was prepared from the results of temperature distribution calculations for the two reference turbines. These maximum temperature differences will be used in estimating the order of magnitude stresses. Note that, while the seal differential results in the larger  $\Delta t$  in hub 0 of the potassium turbine, the interstage differential yields a greater  $\Delta t$  in wheel 1 of the cesium turbine.

Contour plots of the temperatures in hub 0 and 1 and in wheel 1 of the five-stage potassium turbine are shown in Fig. 4. The beneficial effects of segmenting the turbine rotor are evident from the figure.

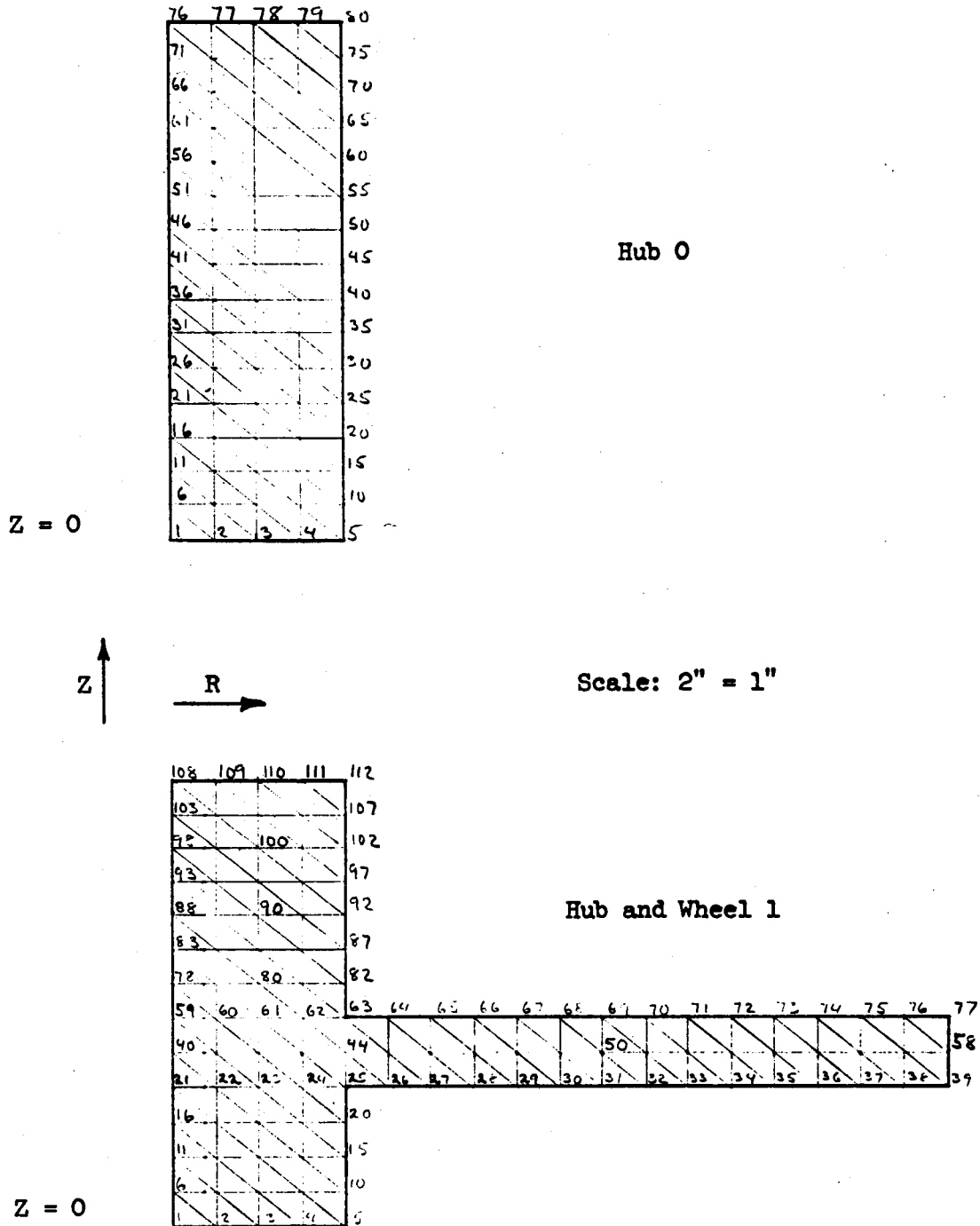


Fig. 2. Finite-Difference Grid for Stress Calculation. 5-Stage Potassium. Nodal Point Identification.

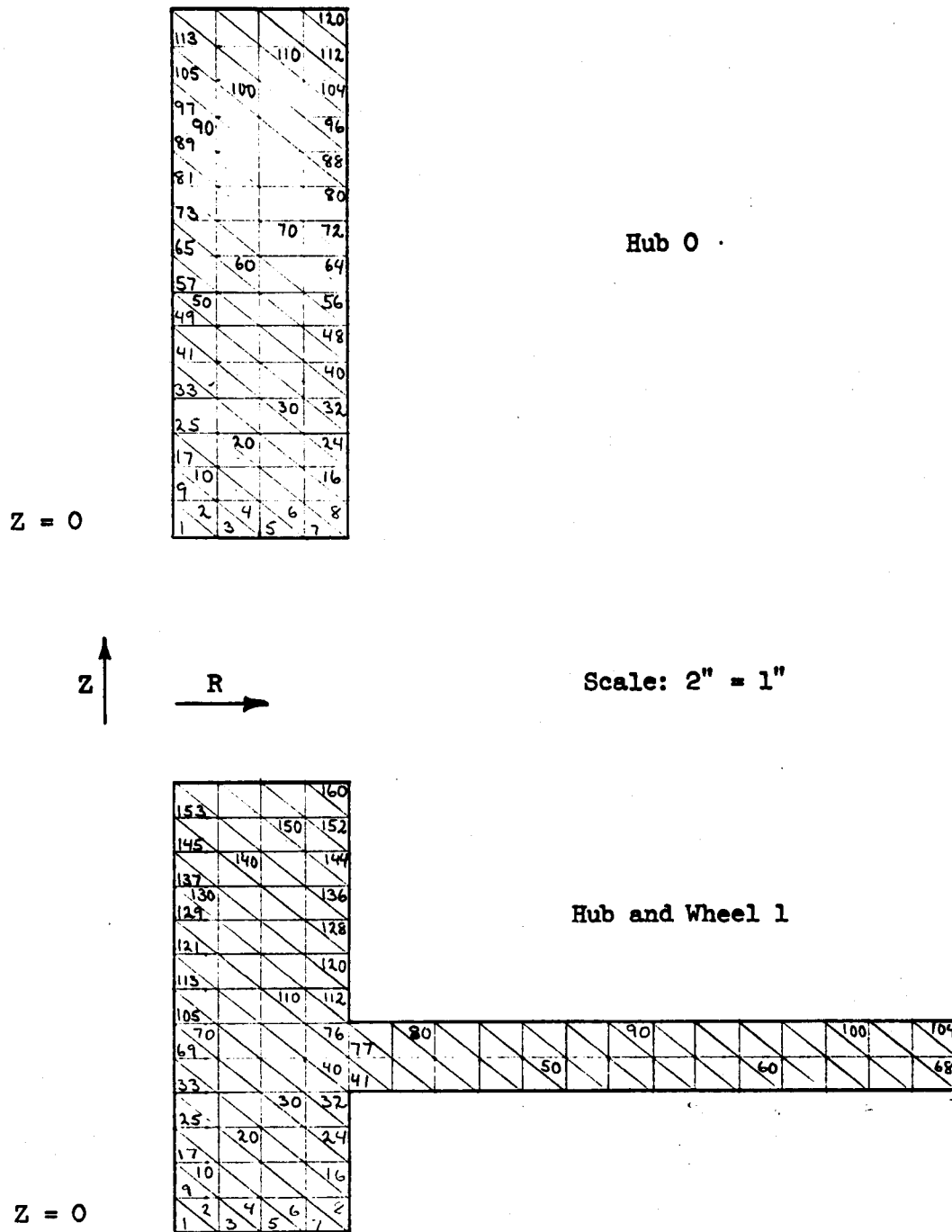


Fig. 3. Finite-Difference Grid for Stress Calculation. 5-Stage Potassium. Element Identification.

Table 1. Maximum  $\Delta t$ 's for Order  
of Magnitude Stress Estimates

	2-Stage Cs (°F)	5-Stage K (°F)
Hub 0	44	149
1	48	39
2	23	37
3	1	28
4		30
5		39
6		1
Seal 1	410	660
Wheel 1	84	32
2	8	4
3		4
4		5
5		16
Bolt	117	160

Roughly a 350°F differential exists between the two hubs, considerably diminishing the gradient the hubs must sustain.

Figure 5 shows the estimated effect on temperature distribution in wheel 1 of imposing the stagnation temperature rise in the vapor adjacent to the upstream corner of the wheel. The circumferential component of nozzle spouting velocity and the wheel peripheral speed resulted in a 141°F rise. While the temperatures and gradients have increased throughout the wheel, note that the maximum gradient near the base of the wheel has been only slightly affected.

An attempt was made to assess the importance of rotor segmentation by running a case with an effectively solid rotor. This was done by setting the contact resistance to a very low value ( $h_c$  very large) in the existing program. As expected, thermal gradients were increased substantially over those observed for the segmented rotor. Unfortunately, this modification had a distinctly destabilizing influence on the iteration and the calculation was terminated on number of iterations while the temperature change per iteration was still unacceptably large. Consequently, no stresses were calculated for this case.

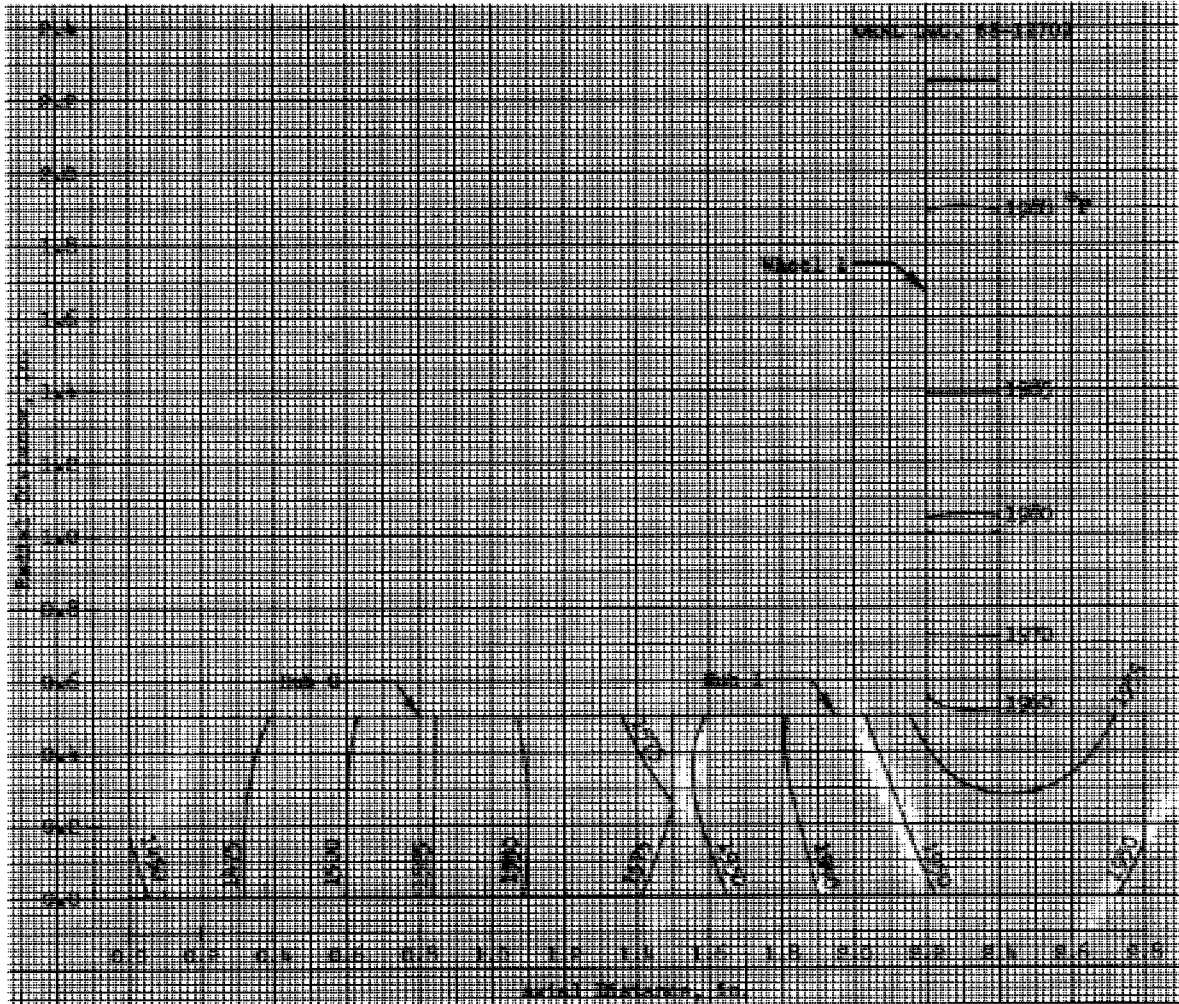


Fig. 4. Isotherms in First Two Hubs and First Wheel of Five-Stage Potassium Turbine.

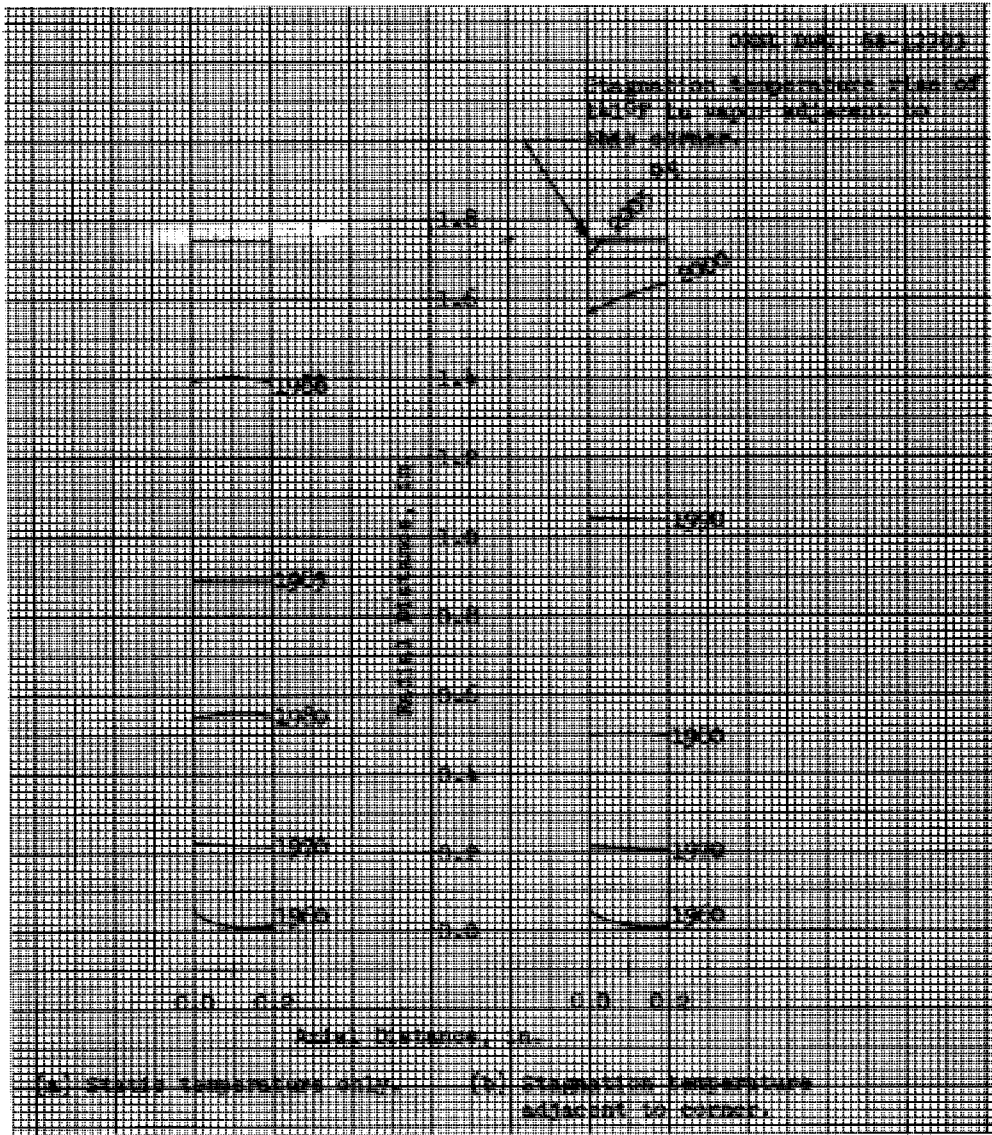


Fig. 5. Effect of Vapor Stagnation Temperature on Temperature Distribution in First Wheel of Five-Stage Potassium Turbine.

StressesHubs and Seals

For hub 0 of the potassium turbine,  $a = 1.0$ ,  $b = 1.5$ ,  $h = 0.5$ , and  $\Delta t = 149$ .  $E\alpha = 97.5$  for all components. Then, the estimated stress is given by

$$\begin{aligned}\sigma_{\max} &= (-0.33)(97.5)(149)(0.707)/1.5 \\ &= -2260 \text{ psi} .\end{aligned}\tag{8}$$

To this thermal stress we must add the compressive stress induced by the bolting forces. The total estimated maximum stress then becomes

$$\sigma_{\max} = -1493 - 2260 = -3753 \text{ psi} .\tag{9}$$

For the first seal, we have  $a = 1.4$ ,  $b = 1.5$ ,  $h = 0.3$ , and  $\Delta t = 660$ . Then, the estimated maximum stress is

$$\begin{aligned}\sigma_{\max} &= (-0.33)(97.5)(660)[\sqrt{(1.40)(0.3)}]/1.5 \\ &= -9175 \text{ psi} .\end{aligned}\tag{10}$$

Analysis of hub 0 by means of the SAFE-PCRS code yielded a maximum element stress in the axial direction of  $-2014$  psi. The order-of-magnitude estimate is thus seen to be conservative by a factor of about 1.86.

Figure 6 is a contour plot of the nodal point axial stresses for hub 0. The stresses are compressive throughout and of the order of 1500 psi over a major portion of the hub. This value is close to the stress arising from the bolting force alone, indicative of a rather small thermally induced stress. The isotherms in Fig. 4 are consistent with this latter conclusion, showing only slight curvature and displaying an almost linear axial variation over the central portion of hub 0.

Wheels

Wheel 1 of the cesium turbine has the larger  $\Delta t$ , so that we have, with  $\Delta t = -84$  (inner temperature less than outer),

$$\sigma_{\max} = (97.5)(-84)/1.4 = -5850 \text{ psi} .\tag{11}$$

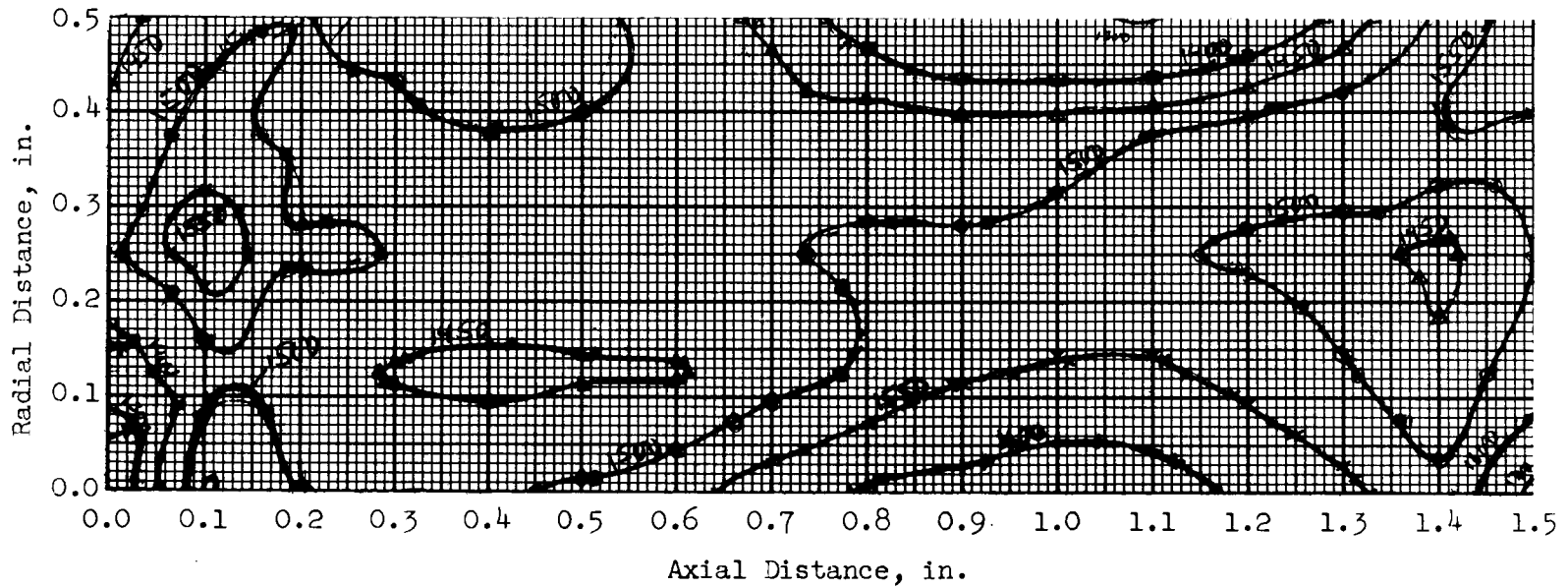


Fig. 6. Axial Stress Contours for Hub 0 of Five-Stage Potassium Turbine. Plotted from Nodal Point Stresses of SAFE-PCRS Program.

The corresponding stress for the potassium turbine (for comparison with SAFE-PCRS) is -2229 psi with a  $\Delta t = -32^\circ\text{F}$ .

The finite-element analysis of the potassium turbine wheel 1 gave a maximum element stress of about -1200 psi. Thus, although possibly by happenstance, the ratio of estimated to computed stresses is again very near to 1.86.

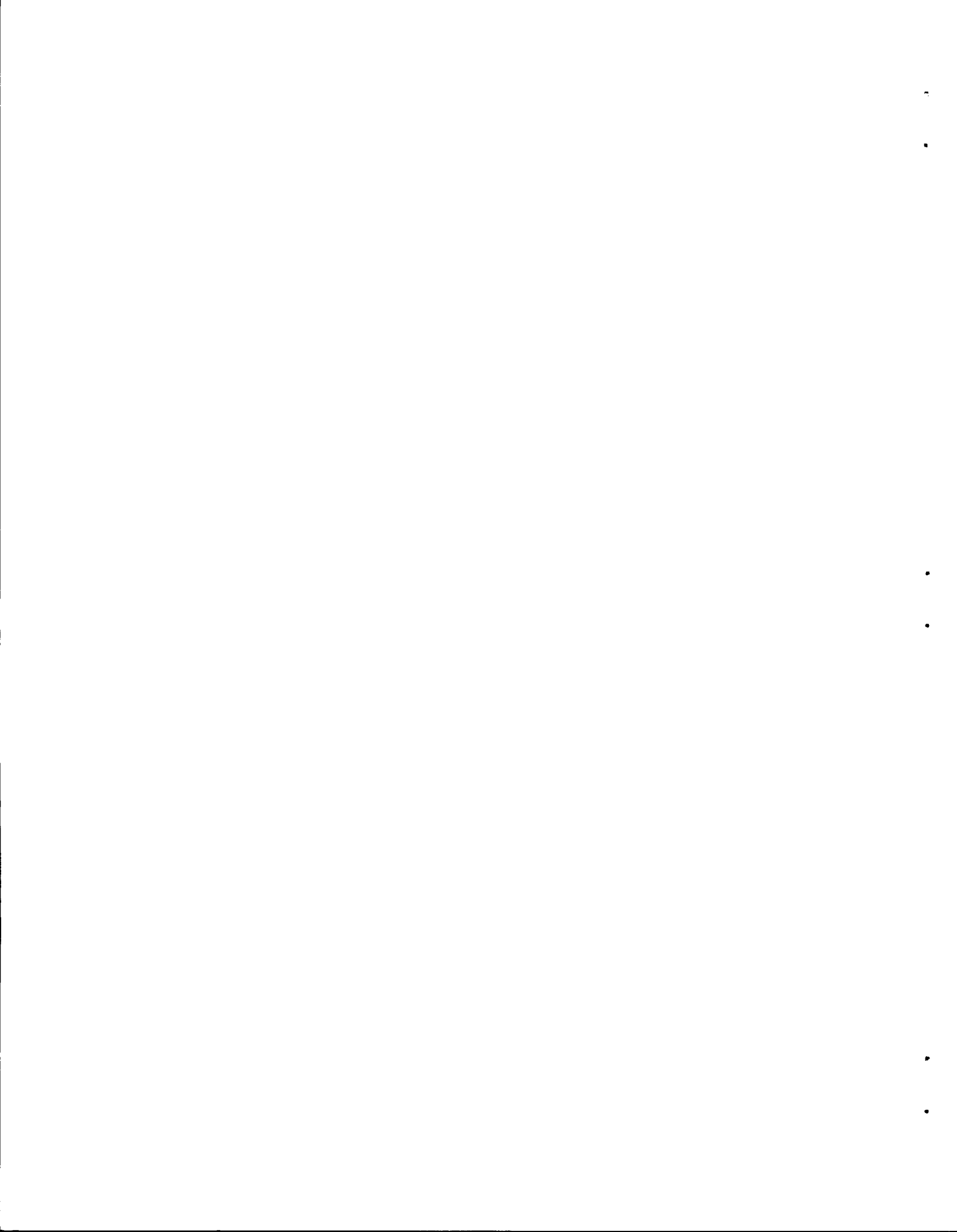
### Bolt

The potassium turbine has the larger bolt  $\Delta t$ ,  $-160^\circ\text{F}$ . We then get an upper limit on the bolt stress of

$$\sigma_{\max} = (97.5)(-160)/2 = -7800 \text{ psi} . \quad (12)$$

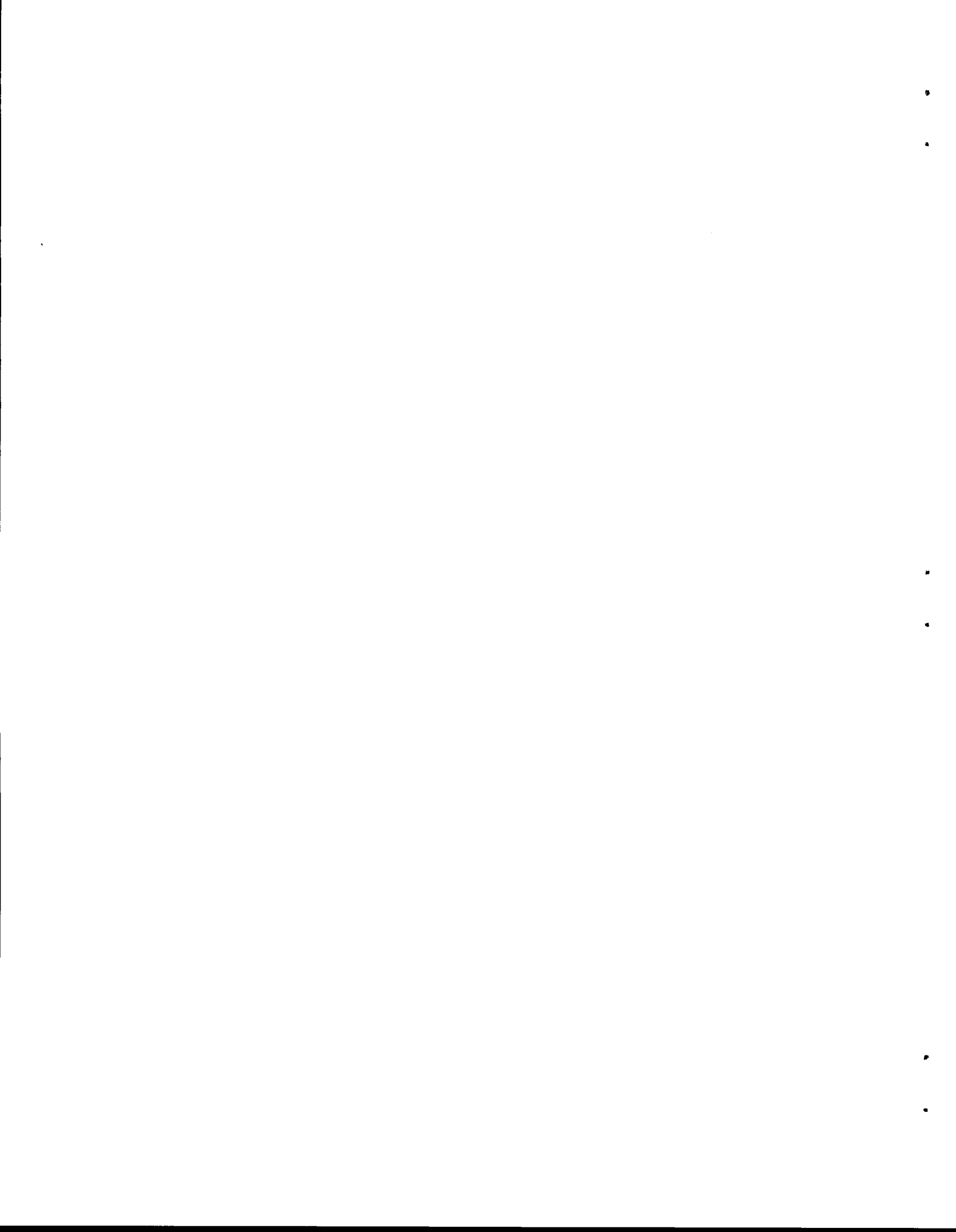
The bolting forces are tensile here, yielding a countering stress of 2654 psi after allowing for the difference in bolt and hub cross-sectional areas. The net estimated stress for the bolt is then

$$\sigma_{\max} = 2654 - 7800 = -5146 \text{ psi} . \quad (13)$$



References

1. A. P. Fraas, D. W. Burton and L. V. Wilson, Design Comparison of Cesium and Potassium Vapor Turbine-Generator Units for Space Power Plants, USAEC Report ORNL-TM-2024, Oak Ridge National Laboratory (AEC Interagency Agreement 40-98-66, NASA Order W-12,353)(to be published).
2. W. L. Stewart, Analytical Investigation of Multistage-Turbine Efficiency Characteristics in Terms of Work and Speed Requirements, NACA-RM E57K22b, Lewis Flight Propulsion Laboratory, February 1958.
3. E. Schnetzer, Comparison Study of Cesium and Potassium for Rankine Cycle Space Power Systems, TMS Report No. 67-1, General Electric Space Power and Propulsion Section, July 1966.
4. D. C. Cornell and Y. R. Rashid, SAFE-PCRS, A Computer Program for the Stress Analysis of Composite Bodies of Revolution. Input Instructions, USAEC Report GA-6588, General Atomic, Aug. 1, 1965.
5. A. P. Fraas, A. G. Grindell and H. C. Young, Survey of Information on Turbine Bucket Erosion, USAEC Report ORNL-TM-2088, Oak Ridge National Laboratory (AEC Interagency Agreement 40-98-66, NASA Order W-12,353)(to be published).
6. S. Timoshenko and S. Woinowsky-Krieger, Theory of Plates and Shells, 2nd edition, pp. 497-501, McGraw-Hill, New York, 1959.
7. R. Daane, Thermal Stress and Distortion, p. 9-111 in Nuclear Engineering Handbook, ed. by H. Etherington, McGraw-Hill, New York, 1958.
8. R. W. Clough and Y. Rashid, Finite Element Analysis of Axisymmetric Solids, Proc. ASCE, J. Eng. Mech. Div., 91(EML): 71-85 (February 1965).



## INTERNAL DISTRIBUTION

- |       |                       |        |  |
|-------|-----------------------|--------|--|
| 1.    | S. E. Beall           | 44.    | R. N. Lyon                                   |
| 2.    | D. L. Burton, ORGDP   | 45.    | R. E. MacPherson                             |
| 3.    | D. L. Clark           | 46.    | H. C. McCurdy                                |
| 4.    | W. B. Cottrell        | 47.    | J. W. Michel                                 |
| 5.    | F. L. Culler          | 48.    | A. J. Miller                                 |
| 6.    | J. H. DeVan           | 49.    | A. M. Perry                                  |
| 7.    | J. R. DiStefano       | 50.    | T. T. Robin                                  |
| 8.    | B. Fleischer          | 51.    | M. W. Rosenthal                              |
| 9-28. | A. P. Fraas           | 52.    | G. Samuels                                   |
| 29.   | A. G. Grindell        | 53.    | A. W. Savolainen                             |
| 30.   | W. O. Harms           | 54.    | M. J. Skinner                                |
| 31.   | P. N. Haubenreich     | 55.    | I. Spiewak                                   |
| 32.   | H. W. Hoffman         | 56.    | D. B. Trauger                                |
| 33.   | R. S. Holcomb         | 57.    | A. M. Weinberg                               |
| 34.   | W. R. Huntley         | 58.    | G. D. Whitman                                |
| 35.   | D. H. Jansen          | 59.    | L. V. Wilson                                 |
| 36.   | P. R. Kasten          | 60-69. | H. C. Young                                  |
| 37.   | R. L. Klueh           | 70.    | ORNL Patent Office                           |
| 38.   | M. E. Lackey          | 71-72. | Central Research Library                     |
| 39.   | J. A. Lane            | 73-74. | Y-12 Document Reference Section<br>(DRS)     |
| 40.   | W. J. Larkin, AEC-ORO | 75-94. | Laboratory Records (LRD)                     |
| 41.   | M. E. LaVerne         | 95.    | Laboratory Records - Record Copy<br>(LRD-RC) |
| 42.   | A. P. Litman          |        |  |
| 43.   | M. I. Lundin          |        |  |

## EXTERNAL DISTRIBUTION

96. J. J. Lynch, RNP, NASA, Washington, D.C.  
97-106. S. V. Manson, RNP, NASA, Washington, D.C.  
107. F. Schulman, RNP, NASA, Washington, D.C.  
108. W. H. Woodward, RN/D, NASA, Washington, D.C.  
109. R. L. Cummings, SPSD, NASA-LRC, Cleveland, Ohio  
110. R. E. English, SPSD, NASA-LRC, Cleveland, Ohio  
111. J. A. Heller, SPSD, NASA-LRC, Cleveland, Ohio  
112. B. Lubarsky, SPSD, NASA-LRC, Cleveland, Ohio  
113. T. P. Moffitt, FSCD, NASA-LRC, Cleveland, Ohio  
114. T. A. Moss, SPSD, NASA-LRC, Cleveland, Ohio  
115. L. Rosenblum, M&SD, NASA-LRC, Cleveland, Ohio  
116. W. L. Stewart, FSCD, NASA-LRC, Cleveland, Ohio  
117. R. N. Weltmann, SPSD, NASA-LRC, Cleveland, Ohio  
118. N. Grossman, DRD&T, AEC, Washington, D.C.  
119. C. Johnson, SNS, AEC, Washington, D.C.  
120. G. Leighton, SNS, AEC, Washington, D.C.  
121. O. E. Dwyer, Brookhaven National Laboratory, Upton, N.Y.  
122. D. H. Gurinsky, Brookhaven National Laboratory, Upton, N.Y.  
123. J. Hadley, Lawrence Radiation Laboratory, Livermore, California  
124. D. R. Bartz, Jet Propulsion Laboratory, Pasadena, California

125. J. Davis, Jet Propulsion Laboratory, Pasadena, California
126. D. Elliot, Jet Propulsion Laboratory, Pasadena, California
127. L. Hays, Jet Propulsion Laboratory, Pasadena, California
- 128-131. M. A. Zipkin, General Electric Company, Cincinnati, Ohio
- 132-133. R. D. Gruntz, AiResearch, Phoenix, Arizona
- 134-135. W. D. Puchot, Astronuclear Lab., Westinghouse Electric, Pittsburgh, Pennsylvania
- 136-137. V. R. Degner, Rocketdyne Division, N.A.A., Canoga Park, California
- 138-139. R. Gordon, SNAP-8 Division, Aerojet-General, Azusa, California
140. R. H. Chesworth, Aerojet-General Nucleonics, San Ramon, California
141. J. Edward Taylor, TRW, Inc., Cleveland, Ohio
142. C. L. Walker, Allison Division of General Motors, Indianapolis, Indiana
143. B. Sternlicht, Mechanical Technology Incorporated, Latham, New York
144. R. Myers, Pratt and Whitney Aircraft Corporation, E. Hartford, Conn.
145. S. Greenberg, Argonne National Laboratory, Argonne, Illinois
146. R. L. Eichelberger, Atomics International, Canoga Park, California
147. K. Goldmann, United Nuclear Corporation, White Plains, New York
- 148-162. Division of Technical Information Extension (DTIE)
163. Laboratory and University Division (ORO)